How Do Organic Solvents Affect Peroxidase Structure and Function? †

Keungarp Ryu and Jonathan S. Dordick*
Department of Chemical and Biochemical Engineering and Center for Biocatalysis and Bioprocessing, University of Iowa, Iowa City, Iowa 52242

Received August 5, 1991; Revised Manuscript Received December 10, 1991

ABSTRACT: The effect of organic solvents on horseradish peroxidase structure and function has been studied. Some, but not complete, enzyme denaturation occurs even in low volumes of water-miscible organic solvents (e.g., >30% v/v dioxane, >50% v/v methanol, and >20% v/v acetonitrile) as determined by the decreased difference between the fluorescence of peroxidase's sole tryptophan residue and free L-tryptophan in solution. Absorbance and electron paramagnetic resonance spectroscopies indicate exposure of peroxidase's active site to the organic solvent. This reduces the local polarity in the enzyme's active site and results in stronger hydrogen bonding of phenolic substrates to the enzyme. In extreme cases (e.g., 95% v/v dioxane, 90% v/v acetonitrile, and ethyl and butyl acetate containing 2 and 1% v/v aqueous buffer, respectively), the transition state of the enzymic reaction is sufficiently perturbed so as to alter the magnitude of the Hammett ρ value. This is most likely the result of the increased strength of hydrogen bonding between electron-donating alkoxyphenols (negative σ values) and an electrophilic group in the enzyme's active site, thereby reducing catalytic efficiencies for such substrates relative to alkyl- and chlorophenols. Perhaps the most important effect of the organic solvent, however, is the significant ground-state stabilization of phenolic substrates in organic media as opposed to aqueous buffer. This stabilization can account for nearly 4 orders of magnitude in reduction of catalytic efficiency and is manifested in increased K_m's. This study indicates that enzymes can maintain much of their native active-site structure in organic media and that the effect of solvent on substrate thermodynamics must be considered.

Upon placing an enzyme in a nonaqueous medium, the biocatalyst is subjected to a number of factors that can alter its native, aqueous-based, structure and function (Singer, 1962). The native secondary and tertiary structures of enzymes are maintained by the interaction of several noncovalent forces, including hydrogen bonding, and ionic, hydrophobic, and van der Waals interactions (Tanford, 1961; Schultz & Schirmer, 1979). Disruption of such forces, as a result of addition of organic solvents to an aqueous enzyme solution, can lead to diminished substrate binding and catalytic turnover. For example, studies by Kaufman and Neurath (1949), Inagami and Sturtevant (1960), Fink and Angelides (1976), Tanizawa and Bender (1974), Bender (1987), and Clark and co-workers (Guinn et al., 1991; Fernandez et al., 1991) comprising several hydrolytic enzymes showed that the substrate K_m increased as the organic solvent concentration increased yet catalytic turnover was relatively unaffected below ca. 80% v/v organic solvent. Furthermore, in all cases, little evidence of major enzymic structural change was observed.

As opposed to diminished substrate binding, losses in catalytic turnover have been correlated to bulk structural changes in the enzyme. For example, Mozhaev et al. (1989) reported that both the fluorescence intensity and emission wavelength maximum of chymotrypsin increased sharply toward those of free tryptophan upon addition of 40% 2,3-butanediol to aqueous buffer. A sharp increase in fluorescence intensity accompanied a large drop in V_{max} for the hydrolysis of *N*-benzoyl-L-tyrosine *p*-nitroanilide, suggesting that substantial denaturation of chymotrypsin occurred in this solvent. In addition to glycols, solvents such as 2-chloroethanol and dimethyl sulfoxide (DMSO)[1] cause profound inactivation of enzymes (Herskovits, 1965). A case in point is ribonuclease which upon dissolution in increasing concentrations of 2-chloroethanol undergoes a transition from the native state to a partially unfolded protein to a newly folded, incorrect structure (Weber & Tanford, 1959). In extreme cases, the hydrophobic core of an enzyme becomes exposed to the organic solvent, thereby leading to inactivation (Klysov et al., 1975).

Correlations between enzyme structure and catalytic activity, however, require direct measurement of active-site structure and the effect of the reaction medium on the transition state of the reaction. Such information has been gleaned from kinetic, structural, and dynamic studies. Kanerva and Klibanov (1989) studied subtilisin-catalyzed hydrolysis and transesterification of substituted phenyl acetates in water and several organic solvents. Hammett coefficients (ρ) of subtilisin catalysis in water and organic media were identical, suggesting that the active site was predominantly shielded from the bulk organic solvent and that the solvent did not affect the transition-state structure of the reaction. This was confirmed by structural analysis of a related enzyme, α-lytic protease from *Lysobacter enzymogenes*, via solid-state ^{15}N-NMR (Burke et al., 1989). Finally, the role of water in controlling active-site structure and dynamics of subtilisin Carlsberg catalysis has been probed by conventional and saturation-transfer EPR (Affleck et al., 1992). Increased molecular motion of a spin label bound to the active-site Ser_{221} of subtilisin as water is added to tetrahydrofuran suggests that water increases active-site flexibility. Water also was shown to increase the

† This work was supported by the National Science Foundation (Grants CBT-8808897 and BCS-8958415, PYI award to J.S.D.) and by the Mead Corp. Acknowledgment is made to the donors of the Petroleum Research Fund, administered by the American Chemical Society, for support of this work. K.R. was supported in part by a fellowship from Eastman Kodak.

* To whom correspondence should be addressed.

[1] Abbreviations: DMSO, dimethyl sulfoxide; DMF, *N*,*N*-dimethylformamide; HRP, horseradish peroxidase; HPLC, high-performance liquid chromatography; EPR, electron paramagnetic resonance; τ, rotational correlation time(s) of spin-label; *N*-Ac-L-Trp-NH_2, *N*-acetyl-L-tryptophanamide.

0006-2960/92/0431-2588$03.00/0

active-site polarity, thereby indicating that water may form condensate in the active site of subtilisin and increases flexibility presumably by dielectric screening of the charged/polar groups in the active site.

The aforementioned studies suggest that enzymatic catalysis in organic solvents is possible if the active-site structure is not substantially perturbed by the organic solvent and if enough water is present [although this water content may be as low as a fraction of a monolayer of an enzyme (Zaks & Klibanov, 1986)]. Moreover, despite the enormous interest in using hydrolytic enzymes as catalysts in organic solvents (Dordick, 1989, 1991; Klibanov, 1989, 1990; Laane et al., 1987; Halling, 1987), no systematic evaluation has been carried out on the combined kinetic and structural consequences of nonaqueous reaction media on enzymes that do not use water as a coreactant.

In the present study, horseradish peroxidase has been used to elucidate solvent effects on enzyme structure and function. Peroxidase catalyzes the oxidation of a wide variety of organic compounds in the presence of hydrogen peroxide and does not use water as a coreactant (Saunders et al., 1964; Dunford & Stillman, 1976; Halliwell & De Rycker, 1978). The reaction mechanism is characterized by an initial two-electron oxidation of the native ferric enzyme to an oxidized intermediate (compound I) by hydrogen peroxide. The regeneration of native peroxidase is accomplished by two sequential one-electron reductions through a partially oxidized intermediate (compound II). The peroxidatic cycle, therefore, results in the oxidation of a variety of electron donors such as phenols, aromatic amines, and other reducing equivalents including highly substituted methoxybenzenes (Kersten et al., 1990) (e.g., 1,2,4,5-tetramethoxybenzene) and nonaromatic compounds such as dihydroxyfumaric acid, NADH, and reduced sulfides (e.g., glutathione, cysteine, and dithiothreitol) (Halliwell & De Rycker, 1978). The enzyme contains a protoporphyrin IX group which is held in place by electrostatic interactions between one of the heme's propionic acid side-chains and the apoprotein's Lys_{174} group (Yeoman & Hager, 1980). While the crystal structure of HRP has not been determined, the active-site structure is believed to be similar to cytochrome *c* peroxidase with the Arg_{183} residue in HRP corresponding to Ser_{185} in cytochrome *c* peroxidase (Welinder, 1979; Ortiz de Montellano, 1987; Sakurada et al., 1986). Finally, HRP is an ideal model with which to study. It is catalytically active in organic media (Ryu et al., 1989; Ryu & Dordick, 1989), has a wide specificity with substrates (phenols) that are highly soluble in organic solvents, is commercially available in pure protein form, and has a structural "marker" (i.e., active-site heme group) to aid in the elucidation of solvent-induced structural perturbations of the active site.

Experimental Procedures

Materials. Horseradish peroxidase (type II) was purchased from Sigma Chemical Co. (St. Louis, MO) and used without any further purification. All phenols and solvents used in this work were purchased from Aldrich (Milwaukee, WI) and were of the highest quality commercially available. All solvents were bi-distilled prior to use, and 1,4-dioxane was further purified by the method of Wiberg (1960) to remove trace organic peroxides. The nitroxide spin label (3-carboxy-2,2,5,5-tetramethyl-3-pyrrolinyl-1-oxy *N*-hydroxysuccinimide ester) was purchased from Eastman Kodak Co. (Rochester, NY). Glass beads (75–150 μm) were purchased from Sigma.

Peroxidase Kinetics in Soluble Form. The initial rates of phenolic oxidations catalyzed by peroxidase were followed by spectrofluorometry (Shimadzu RF-5000 spectrofluorophotometer) and HPLC. The excitation and emission λ_{max} values for each phenol oxidation product were determined by scanning an oxidized (via action by 1 μg/mL HRP and 0.25 mM H_2O_2 for 1 h) solution of a phenol in a given solvent. Absolute kinetic rates were obtained by comparing the increase in fluorescence intensity at λ_{max} to the decrease in phenolic monomer concentration following oxidation by peroxidase using HPLC. The HPLC system employed reverse-phase (C_{18}) μ-Bondapak (Waters, Milford, MA) separation with an eluant of aqueous CH_3CN (45–70% v/v, depending on the phenol studied). Detection was performed at 280 nm with a photodiode array detector (Model 990, Waters). In a typical kinetic experiment, 2 mL of aqueous buffer (10 mM phosphate, pH 7.0) or an aqueous buffer/organic solvent mixture containing a phenol and H_2O_2 (0.25 mM as final concentration) was placed in a spectrofluorometer cuvette. The reaction was initiated by addition of 1 mL of peroxidase solution (0.01–1 μg/mL) of the same content of organic solvent and the initial rate of phenolic oxidation followed spectrofluorometrically for 30 s at 25 °C. Steady-state kinetic constants, V_{max} and K_m, were obtained by using a nonlinear Michaelis–Menten equation fitting with a nonlinear regression algorithm by Himmelbrau (1970).

Peroxidase Kinetics in Immobilized Form. Peroxidase was deposited onto nonporous glass beads (75–150 μm). The beads were washed for 12 h in 10% (v/v) nitric acid followed by copious washing with water until the water wash had a neutral pH. Two milliliters of peroxidase solution (0.2 mg/mL) in 10 mM phosphate buffer, pH 7.0, was added to 4 g of glass beads. The resulting slurry was dried under rotary vacuum at 20 °C for 1 h until visibly dry and freely flowing beads were obtained. The immobilization procedure did not cause enzyme inactivation as determined by a conventional peroxidase assay in aqueous buffer with guaiacol as substrate (Putter, 1974). The peroxidase bound to glass beads was fully stable for up to 3 weeks at −20 °C. It should be noted that in predominantly aqueous solutions, the peroxidase will desorb from the glass beads; however, in predominantly organic solvents, there is no propensity for the enzyme to desorb, and it remains bound to the glass surface. In a typical reaction, 1–10 μg/mL peroxidase bound to glass beads was added to 15 mL of nonaqueous solution containing a phenol, and 0.25 mM H_2O_2 was added to initiate the reaction. The suspension was shaken in 20-mL glass scintillation vials at 250 rpm at 25 °C. Every minute, 0.5 mL of reaction mixture was removed and diluted with 3 mL of the initial reaction mixture (without enzyme). The diluted sample was analyzed by spectrofluorometry. Initial rates were determined during the first 4 min of the reaction. In both soluble and immobilized peroxidase kinetics, conversions were kept to an equivalent of 25% of the initial concentration of H_2O_2 reacted. Steady-state kinetics were determined as described above for soluble peroxidase.

Spin Labeling of Peroxidase. Spin-labeled peroxidase was prepared in 10 mM Tris buffer, pH 8.0, containing 20% (v/v) 2-propanol followed a general method by Clark et al. (1988). To 5 mL of 80% 2-propanol solution was added 15 mg of the spin label 3-carboxy-2,2,5,5-tetramethyl-3-pyrrolinyl-1-oxy *N*-hydroxysuccinimide ester and dissolved by vigorous vortexing. The spin-label solution was added to 15 mL of aqueous buffer containing 20 mg of peroxidase, and the enzyme solution was stirred for 12 h at 4 °C. The low temperature was necessary to modify only surface lysine residues of HRP (Ugarova et al., 1979). The reaction mixture was then centrifuged to remove insoluble materials and subjected to ultrafiltration (Amicon YM5 membrane, molecular weight cutoff of 5000)

by washing with 10 mM phosphate buffer, pH 7.0, until no free spin label was detected in the eluent buffer (via absorbance at 230 nm). The spin-labeled enzyme solution was freeze-dried and stored at 4 °C. For EPR spectra, the spin-labeled enzyme was immobilized onto glass beads as previously described. Approximately one spin label per two peroxidase molecules was attached by this approach. The spin-labeled enzyme retained nearly all its native activity in aqueous buffer.

Electron Paramagnetic Resonance Studies. Spin-labeled peroxidase's first-order derivative spectra were collected at room temperature using a Brüker EPR spectrometer (Model ESP300) with a frequency of 9.78 GHz, microwave power of 20 mW, receiver gain of 2×10^5, time constant of 327.68 ms, and a scan range of 100 G. Spin-labeled peroxidase adsorbed onto 200-mg glass beads was placed in a glass capillary tube, and 0.6 mL of a given solvent was added. The tube was gently vortexed and equilibrated for 10 min before the spectrum was obtained. The EPR spectrum of the glass beads, alone, was subtracted from the spectra of spin-labeled peroxidase; however, the interference by the glass beads with minimal. EPR spectra of soluble spin-labeled peroxidase (in predominantly aqueous solutions) were obtained in a 275-μL flat cell with a TM cavity.

Depending on the τ value, spin-label mobility can be classified into rapid (0.1–2 ns), slow ($2–10^2$ ns), and very slow ($10^2–10^4$ ns) rotational motions (Likhtenshtein, 1979). For rapid rotational motions, eq 1 was used to calculate τ where

$$1/\tau(s^{-1}) = (2 \times 10^8)/[((h_0/h_{+1})^{0.5} - 1)\Delta H_0] \quad (1)$$

ΔH_0 is the width of the central spectral component in Gauss and h_0 and h_{+1} are the intensities of the spectral components in the center- and low-field regions, respectively (Likhtenshtein, 1979). For slow rotational motions, the value of τ is approximated by comparison of the spectra with computer-generated simulations of slow rotational motion spectra as provided by Kuznetsov et al. (1971).

Low-temperature EPR was collected on a Varian spectrometer (Model 109) at 8 K with a microwave frequency of 9.19 GHz, microwave power of 100 mW, receiver gain of 4×10^4, time constant of 250 ms, and scan range of 4 kG. In 0.3 mL of aqueous buffer, 20 mg of peroxidase was dissolved, and 50 μL of enzyme solution was removed and diluted with 1 mL of an aqueous/organic solvent mixture (dioxane, methanol, or acetonitrile) to reach the final content of organic solvent desired. The resulting enzyme preparations were equilibrated for 10 min followed by addition of 0.5 mL of the solution or suspension to a glass capillary tube and the spectra were measured.

Circular Dichroism Spectroscopy. CD spectra between 220 and 260 nm were collected in aqueous buffer or aqueous/organic mixtures containing 2.4 μM (0.1 mg/mL) soluble peroxidase on an AVIV CD spectrometer (Model 60 DS, Lakewood, NJ). The enzyme solutions were equilibrated at room temperature for 20 min before the spectra were collected. The α-helix content was calculated by the method of Chen et al. (1972).

Visible Spectroscopy. Absorbance spectra of HRP between 320 and 700 nm were determined with 2.4 μM (0.1 mg/mL) enzyme in aqueous buffer and various aqueous/organic mixtures. Soluble peroxidase was employed. The enzyme solutions were equilibrated for 20 min at 25 °C before the spectra were collected on a Beckman UV/vis spectrophotometer (Model DU-64). The possibility of contamination of the native peroxidase spectra with compound I or II if H_2O_2 was still present in the purified dioxane was eliminated by adding 3 mg of *p*-ethoxyphenol per 5 mL of dioxane.

Fluorescence Spectroscopy. The fluorescence of tryptophan residues within the peroxidase was measured at an excitation wavelength of 283 nm. The concentration of peroxidase was 3.6 μM (0.15 mg/mL) in all solutions studied. L-Tryptophan (also at 3.6 μM) was used to measure the fluorescence of non-protein-containing tryptophan. Peroxidase or L-tryptophan was equilibrated for 20 min at 25 °C prior to spectral measurements. Fluorescence spectra of the solvents were subtracted from the spectra that contained enzyme or L-tryptophan. Both fluorescence intensity and the λ_{max} of emission were measured; however, for insoluble enzyme samples (e.g., >60% v/v dioxane, >50% v/v acetonitrile, >80% v/v methanol), only λ_{max} values could be determined.

Measurements of Phenolic Activity Coefficients. Activity coefficients for phenols in water/methanol and water/acetonitrile solutions were calculated by measuring their partition coefficients from the aqueous/organic mixture into isooctane (isooctane is immiscible with water, methanol, and acetonitrile). The activity coefficient of a phenol in an organic solvent relative to that in water is then given by eq 2 (Abraham, 1974) where γ represents the activity coefficient of a

$$\gamma^s/\gamma^w = P_w/P_s \quad (2)$$

phenol in water or an aqueous/organic mixture and P_w and P_s are the partition coefficients of a phenol between water and isooctane and between the solvent mixture and isooctane, respectively. The average values of partition coefficients were measured by dissolving 10–100 mg of a phenol in 5 mL of aqueous buffer or a water/organic mixture and contacting the resulting solution with 5 mL of isooctane. The solutions were shaken for 48 h at 250 rpm at 25 °C. Variations in partition coefficients for different amounts of a phenol were negligible in this concentration range. The phenolic concentration in the aqueous phase was determined by HPLC (see above for details), while the phenolic concentration in the isooctane phase was determined spectrophotometrically at 280 nm with extinction coefficients determined by phenolic standards dissolved in isooctane. In order to obtain activity coefficients for phenols dissolved in water/dioxane mixtures, equilibrium into isooctane was not feasible due to the complete miscibility of dioxane and isooctane. Thus, thermodynamic estimations of activity coefficients of phenols in water/dioxane mixtures were performed using the UNIQUAC model as developed by Abrams and Prausnitz (1975).[2]

RESULTS

Kinetic Studies

The catalytic activity of HRP is dramatically lowered in nonaqueous media. For example, the catalytic efficiency (V_{max}/K_m) of HRP decreases as much as 4 orders of magnitude as the mole fraction of water-miscible organic solvents (e.g., dioxane, methanol, or acetonitrile) increases. The aim of this research was to quantitatively understand the primary causes for this loss in catalytic activity when peroxidase is placed in organic media with different levels of hydration. To that end, we have investigated linear free energy relationships (LFER's) between substrate structure and peroxidase's catalytic efficiency in a number of organic solvents containing various degrees of hydration. Phenols substituted at either the para

[2] The application of the UNIQUAC thermodynamic model required the calculation of the van der Waals volume and surface area of the solvent, phenol, and phenolic substituent with data from Sorensen and Arlt (1980). A full thermodynamic analysis of peroxidase catalysis is in preparation (Ryu and Dordick, unpublished results).

Table I: Hydrophobicity and Electronic Parameters of Substrates Used in This Work[a]

phenols	π	σ
p-CH_3	0.56	−0.17
m-CH_3	0.56	−0.07
p-C_2H_5	1.00	−0.15
p-C_3H_7	1.55	−0.13
p-C_4H_9	1.98	−0.20
p-Cl	0.71	0.23
m-Cl	0.71	0.37
p-OCH_3	−0.02	−0.27
p-OC_2H_5	0.38	−0.24
m-OC_2H_5	0.38	0.10
p-OC_3H_7	1.05	−0.25
p-OC_4H_9	1.55	−0.32

[a] Data from Hansch and Leo (1979).

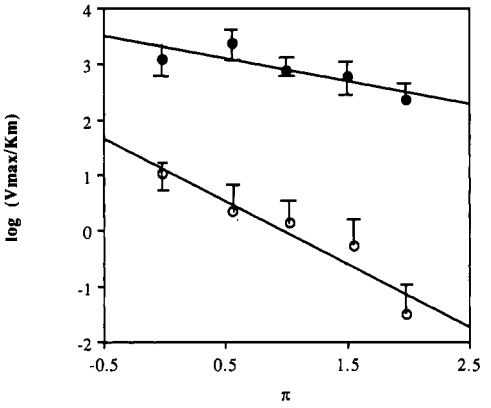

FIGURE 1: Effect of substrate hydrophobicity (π) on the catalytic efficiency of HRP in (●) aqueous buffer and (○) butyl acetate containing 1% aqueous buffer. A summary of the δ values is given in Table II. Phenol concentrations ranged from 0.5 mM to 1 M, and saturation kinetics were observed in aqueous buffer and aqueous dioxane solutions (see Figure 2). Peroxidase concentration was varied from 0.1–1 μg/mL in aqueous buffer to 1–10 μg/mL in organic media. The concentration of H_2O_2 was 0.25 mM in all experiments. Values of π for phenolic substrates are given in Table I. Error bars (in this and relevant subsequent figures) indicate the standard deviation of the kinetic measurements, performed in triplicate.

Table II: Hydrophobic (δ) and Hammett (ρ) Values for Peroxidase Catalysis in Organic Media

solvent	$\delta^{a,b}$	ρ^a
aqueous buffer	−0.41	−2.25
30% dioxane		−2.87
40% dioxane		−2.45
60% dioxane		−2.30
70% dioxane	−0.63	−2.01
80% dioxane	−0.70	−2.78
95% dioxane	−0.58	−1.39
40% methanol		−2.82
80% methanol		−3.11
80% acetonitrile		−2.15
90% acetonitrile		−0.78
ethyl acetate (2.6% buffer)	−0.90	−1.54
ethyl acetate (2% buffer)		0.03
propyl acetate (1.5% buffer)	−1.24	
butyl acetate (1% buffer)	−1.13	−1.70

[a] All correlation coefficients were greater than 85% as determined by linear regression. [b] Hydrophobicity effects were studied only in the solvents listed with δ values.

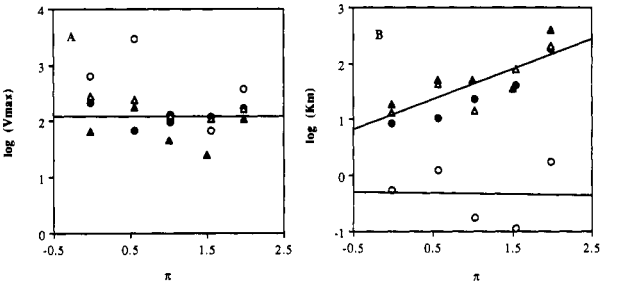

FIGURE 2: Calculated values of individual kinetic constants. (A) Catalytic turnover (V_{max} in micromoles per milligram of HRP per second) as a function of substrate hydrophobicity in (○) aqueous buffer, (●) 70% dioxane, (△) 80% dioxane, and (▲) 95% dioxane. The line through the points is the best fit for nonaqueous media, only. (B) Michaelis constant (K_m in millimolar) as a function of substrate hydrophobicity in the same solvents listed under panel A. The line for nonaqueous media is the best fit for all points. Individual kinetic parameters for phenols in water-immiscible solvents could not be accurately calculated due to the inability to fully saturate the enzyme (approximate K_m values >0.5 M).

or the meta positions were employed as substrates (Table I). ortho substituents were not used because of steric constraints (Dunford & Adeniran, 1986). Correlations of the form depicted in eq 3 were sought to describe quantitatively the effects

$$\log (V_{max}/K_m) \propto \delta\pi + \rho\sigma \quad (3)$$

of substrate hydrophobic (π) and electronic (σ) characteristics on the catalytic efficiency of HRP, where δ and ρ represent the sensitivity and the nature of the hydrophobic and electronic substituent effects, respectively, on HRP catalysis. For reactions with high contents of organic solvents where HRP is insoluble, the enzyme was immobilized onto nonporous glass beads at a loading of 0.1 mg of peroxidase/g of bead. In this manner, internal diffusional limitations were eliminated, and intrinsic enzyme kinetics were obtained in organic media (Ryu et al., 1989). In all reactions, the initial concentration of H_2O_2 was 0.25 mM in order to prevent substrate inhibition. Thus, the kinetic parameters are more accurately described as apparent constants.

Hydrophobic Substituent Effects. In an expansion of our previous work involving HRP catalysis in organic media (Ryu & Dordick, 1989), the effect of substrate hydrophobicity on the catalytic efficiency of peroxidase was studied using a series of para-substituted phenols with hydrophobicities ranging from methoxy to t-butyl. This effectively covered a 2 order of magnitude range in substrate hydrophobicity, whereas the deviation in σ values is small (−0.27 to −0.17). Hence, this initial study was limited to substrate hydrophobicity. Logarithmic correlations (linear in free energy terms) were developed by determining the catalytic efficiency constant (V_{max}/K_m) for each phenol in aqueous buffer, in water/dioxane mixtures, and in alkyl acetate solvents with subsaturating levels of hydration. Figure 1 depicts representative LFER's for aqueous buffer and butyl acetate (containing 1% v/v aqueous buffer). Similar LFER's were also observed (data not shown) for other organic solvents with different hydration levels, and the specific δ values (slopes of V_{max}/K_m vs π) are listed in Table II. In all solvents, catalytic efficiency decreased as substrate hydrophobicity increased (negative δ values), yet this effect became more pronounced (magnitude of δ increased) as solvent hydrophobicity is increased (Table II). A linear correlation that exists for δ as a function of solvent hydrophobicity is depicted in eq 4 where log P represents a measure of solvent

$$\delta = -[0.21 (\log P) + 0.86] \quad (4)$$

hydrophobicity and is the logarithm of the partition coefficient of a given solvent between 1-octanol and water (Laane et al., 1987).

These results indicate that LFER's exist between catalytic efficiency and both substrate and solvent hydrophobicities. In order to elucidate whether these observed kinetic effects were due to changes in catalytic turnover (V_{max}) or enzyme–sub-

strate interactions (K_m), the individual kinetic constants in aqueous buffer and water/dioxane mixtures were measured. As shown in Figure 2, the apparent K_m values in dioxane/water mixtures increased as the substrate hydrophobicity increased, whereas in aqueous buffer, the apparent K_m values remained relatively constant. Furthermore, the K_m values in aqueous/dioxane mixtures were up to 4 orders of magnitude higher than in aqueous buffer. Unlike apparent K_m values, very little deviation was evident in the measurable V_{max} values.

Electronic Substituent Effects. Hammett analysis can be used to evaluate solvent effects on the transition-state structure of HRP catalysis. The ρ value represents the charge distribution in the transition state of the reaction and is highly sensitive to the microenvironment of the transition state as well as to the reaction mechanism, itself. Thus, changes in ρ for HRP catalysis in organic solvents would indicate some solvent penetration into the enzyme's active site. Unlike the methodology employed for substrate hydrophobicity effects, it was not possible to use phenols with different σ values and similar π values as few such phenols exist. Hence, the differences in substrate hydrophobicities were corrected by utilizing the effect of solvent on the hydrophobic sensitivity of a given substrate in a given solvent, δ, and utilizing eq 4. Differences in substrate hydrophobicity were eliminated by normalizing catalytic efficiency values to a hypothetical phenol with a hydrophobic substituent constant of $\pi = 1$ using eq 5. In these expressions,

$$\log (V_{max}/K_m)_{mod} = \log (V_{max}/K_m)_{exp} - \delta(\pi - 1) \quad (5)$$

$(V_{max}/K_m)_{exp}$ is the measured value, and $(V_{max}/K_m)_{mod}$ is the corrected value which is used in the present Hammett analysis in organic solvents. The term $\delta(\pi - 1)$ represents the calculated deviation of a phenol from that of the hypothetical phenol with a hydrophobic substituent constant of $\pi = 1$.

Figure 3 depicts the Hammett analysis of HRP catalysis in aqueous buffer and in several representative water-miscible and -immiscible solvents. The values of log $(V_{max}/K_m)_{mod}$ for each substrate were linearly correlated with their respective σ values, resulting in negative ρ values (Table II). Hence, electron-donating substituents activate peroxidase catalysis both in water and in organic solvents. The magnitude of ρ for water/solvent mixtures was generally similar to that in pure aqueous buffer with the exception of 95% (v/v) dioxane and 90% (v/v) acetonitrile. For example, the average value of ρ in 0–80% dioxane, 40 and 80% methanol, and 80% acetonitrile was -2.44 ± 0.33 while in 95% dioxane and 90% acetonitrile, the values of ρ were -1.39 ± 0.28 and -0.78 ± 0.24, respectively. Thus with the exception of 95% dioxane and 90% acetonitrile, the solvent did not appear to alter the transition-state structure and active-site microenvironment of HRP during phenolic oxidations. In water-immiscible solvents, Hammett analysis showed significant changes in ρ values which were dependent upon the degree of solvent hydration (Table II). For example, in ethyl acetate, the ρ value changed from -1.54 to $+0.03$ when the degree of solvent hydration was reduced from 2.6 to 2.0% (v/v).

The electronic substituent effect on substrate binding and catalytic turnover in aqueous buffer and water-miscible organic solvents was investigated by calculating the apparent V_{max} and K_m values (data not shown). The electronic nature of the substituent affected V_{max} values in all water/dioxane mixtures examined such that alkoxyphenols became progressively poorer substrates than alkylphenols as the dioxane content increased. For example, the ratio of $(V_{max})_{cresol}/(V_{max})_{butoxyphenol}$ in water is 1.1. This ratio increases to 2.5 in 30% dioxane and 10.8 in 95% dioxane. Qualitatively similar results were obtained when *p*-propoxy- and *p*-ethoxyphenols were compared to *p*-cresol. The electronic nature of the substituent also affects the K_m with lower values observed for alkoxyphenols as compared to alkylphenols. Unlike V_{max}, however, the solvent only affects the magnitude of K_m (presumably via hydrophobic interactions as previously described) but does not significantly alter the relative differences in K_m between two or more phenols.

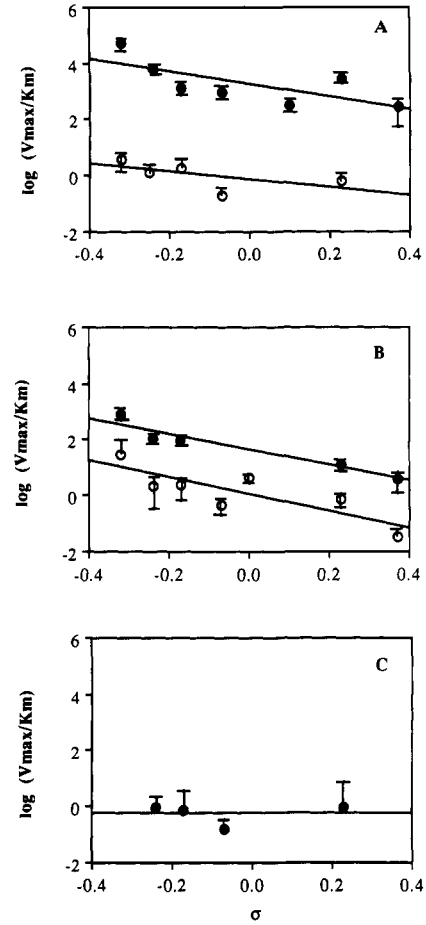

FIGURE 3: Representative Hammett plots for HRP catalysis in (A) (●) aqueous buffer and (○) 95% dioxane, (B) (●) 40% methanol and (○) 80% methanol, and (C) ethyl acetate containing 2% aqueous buffer. Conditions are similar to those described in the legend to Figure 1. Values of σ for phenolic substrates are given in Table I.

Structural Studies

Fluorescence Studies. Fluorescence measurements were conducted to investigate solvent effects on the microenvironment of the single tryptophan residue of peroxidase. This tryptophan residue is not located in the same domain as the active site (Welinder, 1979); however, tertiary structural changes in peroxidase can be inferred from alteration of the tryptophan's microenvironment as determined by fluorescence spectroscopy. Both the fluorescence intensity and maximal emission wavelength (λ_{max}) are sensitive to the polarity and charge densities surrounding the tryptophan residue. Upon denaturation, proteins unfold, and the quantum yield and λ_{max} of tryptophan emission tend toward those of free tryptophan in solution (Teale, 1960; Pajot, 1976). It should be pointed out that free L-Trp was used and not *N*-Ac-L-Trp-NH_2 because of poor solubility of the latter in several organic solvents used.

As shown in Figure 4, in aqueous buffer the λ_{max} and fluorescence intensity of peroxidase are lower than those of free L-tryptophan as is expected for a buried tryptophan residue in a protein (Teale, 1960). In aqueous dioxane mixtures, no change in the λ_{max} or fluorescence intensity was observed up

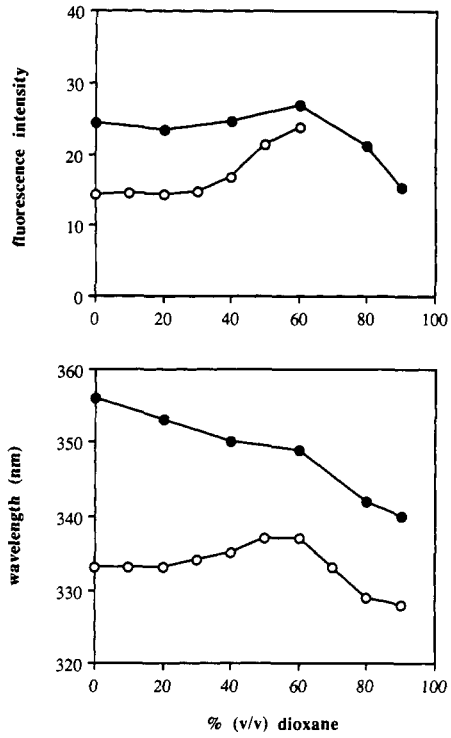

FIGURE 4: Fluorescence intensity (excitation 283 nm, emission at λ_{max}) and λ_{max} of (●) L-tryptophan and (○) HRP in aqueous/dioxane mixtures. Conditions as described under Experimental Procedures.

to 30% v/v (Figure 4). From 30 to 60% v/v, both fluorescence intensity and λ_{max} increased toward those of free L-tryptophan, indicating that the peroxidase underwent some denaturation and the enzyme's tryptophan residue was more accessible to the solvent. Above 60% v/v, the enzyme is not soluble; thus, only λ_{max} can be studied. The peroxidase fluorescence λ_{max} dropped in a manner parallel to that for free L-tryptophan, suggesting that the enzyme's tryptophan residue remained in contact with the reaction medium. Quantitatively similar data were obtained in aqueous methanol and acetonitrile mixtures. For methanol, evidence of protein denaturation was observed above 50% v/v solvent, while with acetonitrile, >20% v/v solvent caused observable denaturation.

Circular Dichroism Studies. Circular dichroism (CD) spectra of soluble peroxidase were obtained from 220 to 260 nm in aqueous solutions of dioxane, methanol, and acetonitrile. In these solvents, virtually no change in the α-helicity of the peroxidase was observed (data not shown). The maximum change occurred in 50% v/v acetonitrile where the α-helix content decreased from 25.8% in aqueous buffer to 21.7%. CD analysis could not be performed in low-water media due to the insolubility of the enzyme. However, the independence in α-helix content with solvent indicates that peroxidase does not lose its native secondary structure in water-miscible organic solvents while remaining soluble.

Soret Absorbance Studies. The characteristic absorption spectrum of native peroxidase shows a major Soret band at 403 nm. Changes in the microenvironment of the heme can shift the wavelength and alter the intensity of the Soret band (Herskovits et al., 1970). For example, dissociation of the heme from the enzyme would result in a blue-shift in the Soret maximum to 398 nm with a concomitant loss in intensity due to dimerization of the dissociated free heme, whereas exposure of the heme to the solvent without dissociation would increase the intensity of the Soret band without shifting the λ_{max}. In water/dioxane and water/methanol mixtures, an increase in the Soret absorbance at 403 nm occurred—as much as 8% in

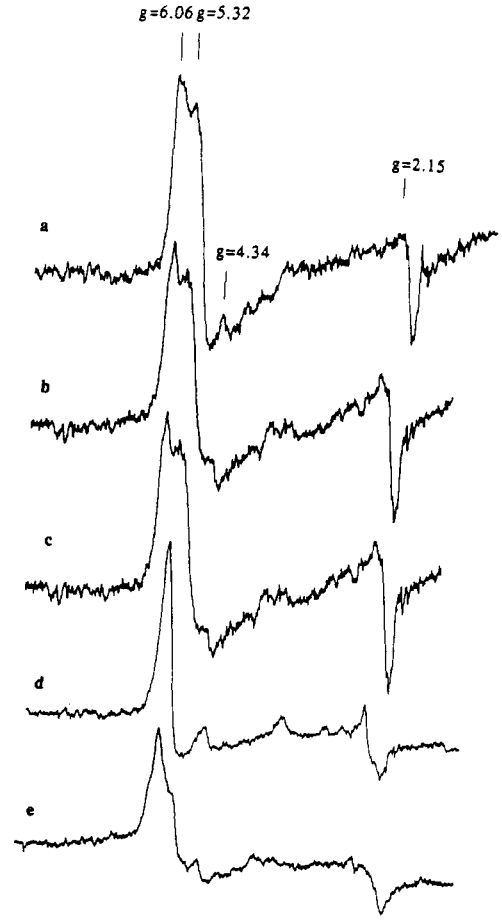

FIGURE 5: EPR spectra of HRP at 8 K in (a) aqueous buffer, (b) 80% dioxane, (c) 95% dioxane, (d) 80% methanol, and (e) 80% acetonitrile. Conditions as described under Experimental Procedures. Very little low-spin iron(III) is observed in dioxane—there are no major signals at g = 2.91, 2.21, and 1.63. Rhombic splitting between g = 6.06 and 5.32 decreased from aqueous buffer to 95% dioxane. In methanol, low-spin iron(III) is evident, and lack of rhombic splitting indicates tetragonal heme symmetry. In acetonitrile, loss of rhombic splitting indicates tetragonal heme symmetry.

70% (v/v) methanol and 9% in 60% (v/v) dioxane—without a shift in λ_{max}, indicative of solvent-induced exposure of the heme to the reaction mixture. In water/acetonitrile mixtures, a broadening of the spectrum below 370 nm and above 425 nm as compared with the spectrum in water was observed. This is most likely due to complexation of the heme iron with the solvent as a ligand, much as with free CN^- (Saunders et al., 1964).

Electron Paramagnetic Resonance Studies. Low-temperature EPR (8 K) can be used to probe solvent effects on the symmetry and spin state of the heme iron in HRP, and thereby directly determine whether the solvent can penetrate into the active site of the enzyme. Native HRP in aqueous buffer, pH 7, exhibits peaks near g = 6 and g = 2 due to the high-spin ferric heme iron, and a rhombic splitting near g = 6 (Blumberg et al., 1968). Figure 5a shows the EPR spectrum of HRP in aqueous buffer (pH 7, 10 mM phosphate) at 8 K. The spectrum exhibits the characteristic ferric iron with rhombic splitting near g = 6, and the g values are 6.06, 5.32, and 2.15. Under these conditions, the rhombicity of the heme iron, as represented by the splitting around g = 6, was calculated to be 4.6% (Δg = 0.74) through the use of eq 6, where R and

$$R = (\Delta g/16)100 \qquad (6)$$

Δg are defined as percent rhombicity and splitting near g = 6, respectively, and is similar to the value of 4.35% obtained

by Blumberg et al. (1968) under similar conditions. Thus, the rhombicity of the heme plane is only 4.6% of maximum.

In either 80 or 95% dioxane solutions, the EPR spectra of peroxidase are not substantially different from that in pure aqueous buffer (Figure 5b,c). The only noticeable difference is in the value of rhombicity which decreased from 4.6 to 3.0% (splitting from 0.74 to 0.48) in going from aqueous buffer to 95% dioxane. The spectrum in aqueous methanol mixtures (80% v/v methanol is shown as an example in Figure 5d) was considerably altered from that in aqueous buffer, and even in 20% v/v methanol, low-spin iron peaks at $g = 2.91$, 2.21, and 1.63 were evident along with a single broad peak at $g = 5.6$, suggesting that the methanol acts as a sixth coordinated ligand to the heme iron. The EPR spectra in aqueous acetonitrile did not show low-spin peaks, and tetragonal symmetry was evident (Figure 5e for 80% v/v acetonitrile).

To probe the dynamics of the entire HRP molecule in organic media, surface spin-labeled HRP was prepared, and the EPR of the spin label was investigated. Figure 6 shows the EPR spin-labeled spectra of HRP in aqueous buffer and in aqueous dioxane mixtures. For comparison, the spectrum of the free spin label is shown. No observable change in the EPR spectra was evident up to 80% v/v dioxane. Above this level of dioxane, the EPR spectra became increasingly broad, and τ increased from 0.6 ns in 80% dioxane to 9 ns in 95% dioxane (legend to Figure 6), indicating reduced spin-label flexibility. Similar results were obtained in methanol above 80% v/v and acetonitrile above 90% v/v. In ethyl and butyl acetates (in the presence of 2.6 and 1% v/v water, respectively), the EPR spectra were rigid (τ of 20 and 9 ns, respectively) (legend to Figure 6).

Discussion

Kinetic Studies. Application of linear free energy relationships to HRP catalysis has provided information about the nature of phenolic binding and catalytic processes. Both hydrophobic and hydrogen-bonding interactions are involved in HRP catalysis, and the reaction medium is expected to affect the magnitude of these individual parameters. It is well-known that substrate specificity and catalytic efficiency depend upon the ability of the enzyme to utilize the free energy of binding with the substrate (Jencks, 1975; Kraut, 1988). This binding energy reflects the difference between binding energies of substrate–enzyme and substrate–solvent interactions (Fersht, 1985). Kinetic parameters describing enzyme function, therefore, depend strongly on the solvent. It may be expected, therefore, that replacement of water with an organic solvent would lead to profound changes in the observed kinetics of enzymatic catalysis due to hydrophobicity changes in the reaction medium that would affect the partitioning behavior of substrates into the enzyme's active site. Furthermore, penetration of the solvent into the active site of an enzyme would be expected to alter the active-site structure as well as the transition-state structure of the reaction by disrupting the fine balance of forces that dictate enzyme and substrate ground-state and transition-state energies in the active site. The hydrophobic nature of substrate binding to the active site of peroxidase has been speculated to be due to the interaction of the phenolic ring with Tyr_{185} of the enzyme (Schejter et al., 1976; Sakurada et al., 1986; Thanabal et al., 1987). The negative slopes (δ values) of catalytic efficiencies vs π (Figure 1 and Table II) indicate that the *p*-alkyl substituents are not in direct contact with hydrophobic amino acids in the active site of HRP and that HRP does not utilize the free energy of hydrophobic interaction with the substrate side chain during catalysis.

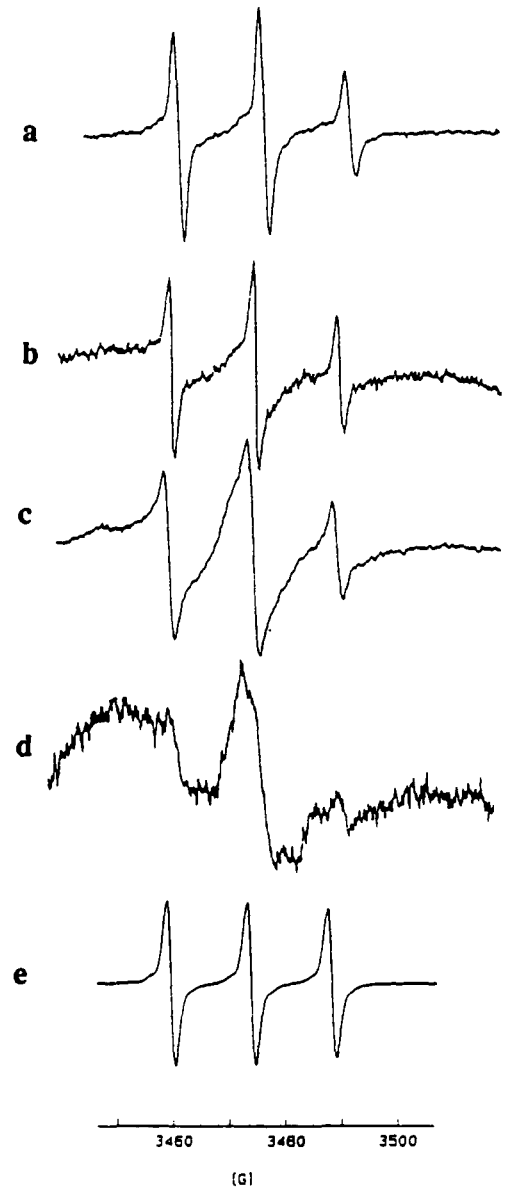

FIGURE 6: Representative EPR spectra of spin-labeled HRP. The spin label 3-carboxy-2,2,5,5-tetramethyl-3-pyrrolinyl-1-oxy *N*-hydroxysuccinimide ester was covalently bound to a surface lysine residue of HRP with an efficiency of one label per two molecules of HRP. The EPR spectrum of free spin label in 100% dioxane is shown for comparison. Spectra in (a) aqueous buffer, (b) 80% dioxane, (c) 90% dioxane, (d) 95% dioxane, and (e) free spin label in 100% dioxane. The τ values of lysine-bound spin label (for all solvents investigated) were 0.7 (aqueous buffer), 0.6 (80% dioxane), 1.3 (90% dioxane), 9.0 (95% dioxane), 0.7 (70% methanol), 1.1 (80% methanol), 2.9 (90% methanol), 0.6 (80% acetonitrile), 6.2 (90% acetonitrile), 20 (ethyl acetate with 2% v/v buffer), and 9.0 (butyl acetate with 1% v/v buffer).

While *p*-alkyl substituents are not directly involved in substrate binding in the enzyme's active site, the hydrophobicities of such substituents can influence the behavior of HRP in organic solvents. For example, the increasingly negative slopes in more hydrophobic organic solvents provide evidence that substrate partitioning, from the bulk reaction medium into the enzymic active site, influences HRP catalysis in organic media. This partitioning is likely to diminish as substrate and solvent hydrophobicity increase, thereby necessitating a larger concentration of substrate to saturate the enzyme and, hence, increased values of the apparent K_m. The observed phenomenon of partitioning is thermodynamically described as either stabilization of the substrate ground state or destabilization

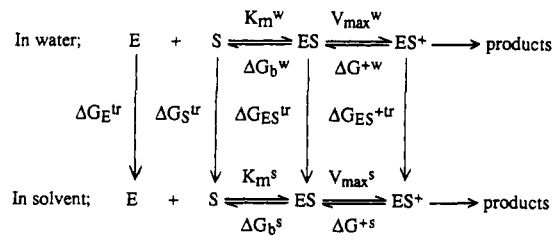

FIGURE 7: Transfer free energies from aqueous to nonaqueous media. Free energy symbols are as described in the text.

of the enzyme–substrate complex.

To determine whether ground-state stabilization or enzyme–substrate complex destabilization caused the substantial increase in the substrate K_m as both substrate and solvent hydrophobicities increased, a free energy analysis of peroxidase catalysis was commenced. Using a transfer free energy method, it is possible to elucidate solvent effects on the free energies of the ground state and enzyme–substrate complex. In addition, such an analysis can be used to quantitatively describe solvent effects on the transition state of the reaction. Figure 7 depicts a simplified kinetic and thermodynamic model for enzymatic catalysis in both water and organic solvents. Transfer free energies (ΔG^{tr}) represent the difference in free energies between water and an organic solvent for enzyme (ΔG_E^{tr}), substrate (ΔG_S^{tr}), enzyme–substrate complex (ΔG_{ES}^{tr}), and transition state (ΔG_{ES}^{+tr}). The transfer free energy for substrate can easily be calculated from thermodynamic relationships (Buncel & Wilson, 1979) using the ratio of activity coefficients in a solvent relative to water (γ_S^s/γ_S^w) where the superscripts s and w represent organic solvent and water, respectively, as shown in eq 7 (note: this is the transfer free

$$\Delta G_S^{tr} = RT \ln (\gamma_S^s/\gamma_S^w) \quad (7)$$

energy of the substrate from water to organic solvent and, hence, the positive sign in the expression). A similar expression for the enzyme is

$$\Delta G_E^{tr} = RT \ln (\gamma_E^s/\gamma_E^w) \quad (8)$$

Substrate binding and catalytic turnover can also be represented in free energy terms using Figure 7 and eq 9 and 10,

$$\Delta G_b^{tr} = RT \ln (K_m^s/K_m^w) = \Delta G_{ES}^{tr} - \Delta G_E^{tr} - \Delta G_S^{tr} \quad (9)$$

$$\Delta G^{+tr} = RT \ln (V_{max}^s/V_{max}^w) = \Delta G_{ES}^{+tr} - \Delta G_{ES}^{tr} \quad (10)$$

where ΔG_b^{tr} and ΔG^{+tr} represent free energy differences between water and an organic solvent for substrate binding and catalytic steps, respectively. Thus, in order to calculate the transfer free energies of the enzyme–substrate complex and transition states, eq 7–10 can be rearranged to give eq 11 and 12 as follows. All values can now be calculated with the

$$\Delta G_{ES}^{tr} = RT \ln (K_m^s/K_m^w) + RT \ln (\gamma_E^s/\gamma_E^w) + RT \ln (\gamma_S^s/\gamma_S^w) \quad (11)$$

$$\Delta G_{ES}^{+tr} = RT \ln (V_{max}^s/V_{max}^w) + RT \ln (K_m^s/K_m^w) + RT \ln (\gamma_E^s/\gamma_E^w) + RT \ln (\gamma_S^s/\gamma_S^w) \quad (12)$$

exception of the activity coefficients for the enzyme in a given solvent (aqueous or organic). However, if we use a series of substrates with systematic structural variations, as was done for the kinetic studies, effects of changes in substrate hydrophobicity on the transfer free energies of the enzyme–substrate complex and transition state can be calculated in a single

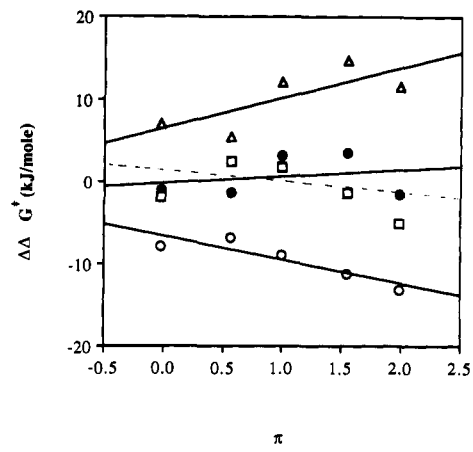

FIGURE 8: Dependence of transfer free energy on substrate hydrophobicity for 70% dioxane. (△) represents the binding step (eq 9), (○) substrate ground state (eq 7), and (●) enzyme–substrate complex (equation 11, enzyme term canceling out) for transfer between aqueous buffer and the solvent indicated. For comparison, the dashed line (□) represents the calculated change in free energy for the enzyme–substrate complex in 95% dioxane.

solvent without knowing the values of enzyme activity coefficients. For a series of substrates in a given solvent, the term $RT \ln (\gamma_E^s/\gamma_E^w)$ cancels out of eq 11 and 12.

Figure 8 shows an example of the dependence of the transfer free energy of the substrate ground state on substrate hydrophobicity, π, in an organic solvent (in this case, 70% dioxane). Free energy changes for the binding step were calculated using eq 9. The transfer free energies of the enzyme–substrate complex were calculated using eq 11. The resulting transfer free energies of the enzyme–substrate complex were invariant to substrate hydrophobicity. Similar results were obtained in 80% dioxane (data not shown). Hence, in these solvents, the decreased binding efficiency of phenols upon an increase in the hydrophobicity of both substituent and solvent was solely due to the enhanced stabilization of phenols in the ground state. As shown in Figure 2, V_{max} values in water/dioxane mixtures were generally insensitive to substrate hydrophobicity. Thus, ΔG_{ES}^{+tr} must also be insensitive to π values. For 95% dioxane, the transfer free energy method shows some evidence for enzyme–substrate complex stabilization (slight negative slope in Figure 8, dashed line), suggesting that the solvent affects the structure of the enzyme's active site.

Hammett analysis has proven to be a powerful tool in elucidating solvent effects on the catalytic events at the active site of HRP. The magnitudes of ρ obtained in this work were smaller than those reported from transient-state kinetic studies. Using stopped-flow methods in aqueous buffer, Job and Dunford (1976) obtained a ρ value of −6.9 for the reactions between HRP compound I and phenols. For the reactions between HRP compound II and phenols, ρ values of −4.6 and −3.8 were obtained by Dunford and Adeniran (1986) and Sakurada et al. (1990), respectively. As noted by Dunford and Adeniran, the smaller magnitude of ρ for compound II reactions as compared to compound I reactions is due to the more complicated reaction mechanism for compound II than compound I. The same rationale can explain the smaller ρ for steady-state kinetics compared to transient kinetics as the apparent V_{max}/K_m encompasses multiple reaction steps including substrate binding and catalysis.

A consequence of solvent penetration into peroxidase's active site is the reduced polarity of the binding pocket in less polar media. Poh (1980) observed that the magnitude of ρ for the dissociation constants of substituted acetic acids, aliphatic

amines, and benzoic acids in aqueous mixtures of dioxane, methanol, and ethanol was inversely proportional to the solvent dielectric constant such that in polar solvents, as compared to nonpolar solvents, the magnitude of the aforementioned ρ values decreased, presumably due to dipole solvation by the solvent. In the present study, however, the magnitude of ρ slightly decreased as solvent polarity is *decreased*, suggesting that in aqueous buffer phenolic substrates may be in a solvated state due to specific interactions in the active site of peroxidase. These interactions become stronger as solvent polarity decreases. In ethyl and butyl acetates with low levels of hydration, and in 95% dioxane and 90% acetonitrile, the solvents are nonpolar, and it may be speculated that the magnitude of ρ is diminished due to stronger hydrogen bonding between the substrate and enzyme. This hypothesis is supported by the dramatic decrease in the magnitude of ρ in ethyl acetate when the water content is decreased from 2.6% to 2.0% v/v (ρ changes from −1.54 to +0.03). Because water contributes significantly to the polarity of an organic solvent, small changes in water content can lead to large changes in the magnitude of ρ.

Low K_m and V_{max} values for the alkoxyphenols as compared to the non-alkoxyphenols imply that strong specific interactions exist between the electron-donating oxygen of the alkoxy substituents and an electrophilic group at the active site of HRP. Sakurada et al. (1986) and Schejter et al. (1976) have suggested that phenolic substrates may form hydrogen bonds with either Arg_{183} or the proximal histidine residue coordinated to the heme. The hydrogen-bonding power will be affected by the dielectric constant of the medium (Prausnitz et al., 1986). In more nonpolar solvents (e.g., as the water content of the solvent decreases), it is expected that hydrogen bonding would strengthen, resulting in stronger binding of alkoxyphenols to HRP. This, in turn, will result in lower values of V_{max}/K_m for alkoxy- vs alkylphenols and reduce the observed magnitude of ρ.

Structural Studies. Horseradish peroxidase appears to maintain its active-site structural integrity in most of the organic solvents tested. The reduced rhombicity of HRP in dioxane indicates that the heme symmetry has become more tetragonal (e.g., more similar to free heme in solution) in character and that the enzyme's heme is in a *less* constricted environment in 95% dioxane as compared to aqueous buffer, although the change was not large. The less constricted heme environment in 95% dioxane is indicative of the heme being exposed, if only slightly, to the solvent. This observation is supported by increased Soret absorbance in aqueous/dioxane mixtures. Herskovits et al. (1970) observed similar increases in the Soret absorbance of cytochrome *c* in methanol, 1-propanol, and *t*-butyl alcohol. These findings were attributed to the exposure of the heme from a buried, hydrophobic environment to a more polar environment. It is important to note that no low-spin iron peaks were observed in dioxane. Therefore, dioxane did not act as a sixth coordinated ligand to the heme iron.

Unlike dioxane, methanol and acetonitrile did interact strongly with the active site of HRP. The broad EPR signal at $g = 6$ in 80% methanol becomes as sharp as that of hemin chloride (Peisach & Blumberg, 1972), indicating that heme symmetry has become completely tetragonal and the heme environment is much more open to the solvent. EPR spectra in water/methanol mixtures suggested that methanol acts as a ligand to the heme iron and changes the spin state of the native HRP to low-spin iron (III) while acetonitrile appears to form a cyano complex with the heme (a finding supported by Soret absorbance measurements).

Fluorescence spectroscopy revealed structural alterations of peroxidase in all solvents tested. In water/dioxane mixtures, no observable fluorescence changes occurred below 30% v/v dioxane. The increase in both fluorescence intensity and λ_{max} above 30% v/v dioxane suggests that the peroxidase undergoes some denaturation that causes the buried tryptophan residue to become accessible to the medium. Above 60% v/v dioxane, both fluorescence intensity and λ_{max} drop, in a manner similar to free L-tryptophan, which shows that the tryptophan remains accessible to the solvent in high concentrations of dioxane. These structural alterations could not be directly correlated to peroxidase kinetics in dioxane as the fluorescence method did not probe directly the active site of the enzyme. Denaturation in water/dioxane mixtures, however, does not significantly affect the active site of HRP as the ρ value is unchanged until 95% (v/v) dioxane is used as solvent. Similar results were obtained with methanol and acetonitrile—enzymic tryptophan accessibility to either solvent was evident above 50% methanol and 20% acetonitrile. These structural changes did not come about because of changes in the secondary structure of HRP as CD spectra were virtually unchanged between aqueous solutions and aqueous/organic mixtures.

Perhaps the most obvious structural effect was the low flexibility of HRP (as determined by the rotational flexibility of a lysine spin label at the surface of the enzyme) in nonpolar media. It is tempting to speculate that peroxidase loses its catalytic activity due to decreased flexibility in nonpolar solvents. Low absolute values of catalytic efficiency and ρ values in nonpolar solvents can be roughly correlated to the high rotational correlation times of the nitroxide spin label (compare Figures 3 and 6, Tables II and III). However, because the nitroxide spin label is attached to a surface lysine residue of peroxidase, the measured decrease in probe flexibility is reflective of the diminished flexibility of the entire peroxidase molecule but says nothing about active-site flexibility.

In conclusion, peroxidase structure and function are affected by the presence of organic solvents. No complete denaturation of the enzyme occurs, even in the most polar organic solvents, and the measurable catalytic activity of the enzyme in low-water media can be attributed to the high degree of native structural integrity of the enzyme's active site. The loss in catalytic efficiency of HRP in organic solvents is a combination of several factors, including the following: (1) The stabilization of the phenolic ground state in organic media as compared to aqueous buffer. This manifests itself in high substrate K_m values in nonpolar media. (2) Penetration of organic solvent into the enzyme's active site which decreases the local polarity and strengthens the hydrogen bonding of substrates to the enzyme. In extreme cases (e.g., 95% dioxane, 90% acetonitrile, and ethyl and butyl acetates), the penetration of solvent causes a loss in the catalytic specificity of peroxidase (magnitude of ρ decreases), presumably due to the solvent directly affecting the transition state of the enzymatic reaction. The enzyme then becomes less sensitive to the electronic characteristics of the substrate. (3) Bulk tertiary structural changes (however, secondary structural changes cannot be ruled out in low-water media that could not be probed by CD) that indirectly alter the structure of the enzyme's active site.

In many respects, the most influential factor is the alteration in reaction thermodynamics in organic vs aqueous media. Nature has not had to deal with HRP functioning in a substantially nonaqueous environment, and although the enzyme appears to function normally (i.e., follows Michaelis–Menten

kinetics) in many organic solvents, it is subjected to unnatural thermodynamic limitations in such solvents. Because HRP is not unique among non-membrane-bound enzymes, it is probable that most other enzymes have similar constraints when used in organic solvents. Through the use of medium design and protein engineering, it may be feasible to improve enzyme function by either destabilizing the substrate ground state or stabilizing the enzyme–substrate complex. The former requires employing a solvent that does not give high substrate solubilities (and hence a tradeoff will exist between activity and productivity), while the latter requires protein engineering to improve enzyme–substrate binding. Both approaches are being examined in continuing work with a number of enzymes. From a practical standpoint, the results of this study have allowed us to develop quantitative and predictive expressions following the form depicted in eq 3. In a simplified model expression, the catalytic efficiency of HRP is shown in eq 13 where values of π, σ, and ρ can be found from Tables I and II.

$$\log (V_{max}/K_m) \propto \rho\sigma - [0.21 (\log P) + 0.86](\pi) \quad (13)$$

Acknowledgments

We thank Drs. C. C. Felix and W. Antholine at the National Biomedical ESR Center, Medical College of Wisconsin, Milwaukee, WI, and Dr. G. R. Buettner at the University of Iowa ESR Facility for use of ESR equipment, and A. R. Pokora at Mead Central Research for useful discussions.

References

Abraham, M. H. (1974) *Prog. Phys. Org. Chem. 11*, 2.
Abrams, D. S., & Prausnitz, J. M. (1975) *AIChE J. 21*, 116.
Bender, M. L. (1987) *Methods Enzymol. 135*, 537.
Blumberg, W. E., Peisach, J., Wittenberg, B. A., & Wittenberg, J. B. (1968) *J. Biol. Chem. 243*, 1854.
Buncel, E., & Wilson, H. (1979) *Acc. Chem. Res. 12*, 42.
Burke, P. A., Smith, S. O., Bachovchin, W. W., & Klibanov, A. M. (1989) *J. Am. Chem. Soc. 111*, 8290.
Chen, Y. H., Yang, J. T., & Martiner, H. M. (1972) *Biochemistry 11*, 4120.
Clark, D. S., Skerker, P. S., Creagh, L., Guinn, R. M., Prausnitz, J., & Blanch, H. W. (1988) *ACS Symp. Ser. 392*.
Dordick, J. S. (1989) *Enzyme Microb. Technol. 11*, 194.
Dordick, J. S. (1991) in *Applied Biocatalysis* (Blanch, H. W., & Clark, D. S., Eds.) pp 1–51, Marcel Dekker, New York.
Dunford, H. B., & Stillman, J. S. (1976) *Coord. Chem. Rev. 19*, 187.
Dunford, H. B., & Adeniran, A. (1986) *Arch. Biochem. Biophys. 251*, 536.
Fernandez, M. M., Clark, D. S., & Blanch, H. W. (1991) *Biotechnol. Bioeng. 37*, 967.
Fersht, A. (1985) *Enzyme Structure and Mechanism*, 2nd ed., W. H. Freeman and Co., New York.
Fink, A. L., & Angelides, K. J. (1976) *Biochemistry 15*, 5287.
Guinn, R. M., Blanch, H. W., & Clark, D. S. (1991) *Enzyme Microb. Technol. 13*, 320.
Halling, P. J. (1987) *Biotechnol. Adv. 5*, 47.
Halliwell, B., & de Rycker, J. (1978) *Photochem. Photobiol. 28*, 757.
Hansch, C., & Coats, E. (1970) *J. Pharm. Sci. 59*, 731.
Hansch, C., & Leo, A. (1979) *Substituent Constants for Correlation Analysis in Chemistry and Biology*, Wiley-Interscience, New York.
Herskovits, T. T. (1965) *J. Biol. Chem. 240*, 628.
Herskovits, T. T., Gadegbeku, B., & Jaillet, H. (1970) *J. Biol. Chem. 245*, 2588.
Himmelbrau, D. M. (1970) *Process Analysis by Statistical Methods*, John Wiley & Sons, New York.
Inagami, T., & Sturtevant, J. (1960) *Biochim. Biophys. Acta 38*, 64.
Järv, J., Kesvatera, T., & Aaviksaar, A. (1976) *Eur. J. Biochem. 67*, 315.
Jencks, W. P. (1975) *Adv. Enzymol. Relat. Areas Mol. Biol. 43*, 219.
Job, D., & Dunford, H. B. (1976) *Eur. J. Biochem. 66*, 607.
Kanerva, L. T., & Klibanov, A. M. (1989) *J. Am. Chem. Soc. 111*, 6864.
Kaufman, S., & Neurath, H. (1949) *J. Biol. Chem. 180*, 181.
Kersten, P. J., Kalyanaraman, B., Hammel, K. E., Reinhammar, B., & Kirk, T. K. (1990) *Biochem. J. 268*, 475.
Klibanov, A. M. (1989) *Trends Biotechnol. 14*, 141.
Klibanov, A. M. (1990) *Acc. Chem. Res. 23*, 114.
Klysov, A. A., Van Niet, N., & Berezin, I. V. (1975) *Eur. J. Biochem. 59*, 3.
Kraut, J. (1988) *Science 242*, 533.
Kuznetsov, A. N., Wasserman, A. M., Volkov, A. U., & Korst, N. N. (1971) *Chem. Phys. Lett. 12*, 103.
Laane, C., Tramper, J., & Lilly, M. D., Eds. (1987) *Biocatalysis in Organic Media*, Elsevier, Amsterdam.
Likhtenshtein, G. I. (1979) *Spin Labeling Methods in Molecular Biology*, Wiley-Interscience, New York.
Morgenstern, L., Recanatini, M., Klein, T. E., Steinmetz, W., Yang, C., Langridge, R., & Hansch, C. (1987) *J. Biol. Chem. 262*, 10767.
Mozhaev, V. V., Khmelnitskii, Y. L., Sergeeva, M. V., Belova, A. B., Klyachko, N. L., Levashov, A. V., & Martinek, K. (1989) *Eur. J. Biochem. 184*, 597.
Ortiz de Montellano, P. R. (1987) *Acc. Chem. Res. 20*, 289.
Pajot, P. (1976) *Eur. J. Biochem. 63*, 263.
Peisach, J., & Blumberg, W. E. (1972) *Structure and Function of Oxidation–Reduction Enzymes* (Aokeson, A., & Ehrenberg, A., Eds.) pp 191–203, Pergamon Press, New York.
Poh, B. L. (1980) *Aust. J. Chem. 33*, 1175.
Prausnitz, J. M., Lichtenthaler, R. N., & de Azevedo, E. G. (1986) *Molecular Thermodynamics of Fluid Phase Equilibria*, 2nd ed., Prentice-Hall, Englewood Cliffs, NJ.
Putter, J. (1974) in *Methods of Enzymatic Analysis* (Bergmeyer, H. N., Ed.) pp 685–690, Academic Press, New York.
Ryu, K., & Dordick, J. S. (1989) *J. Am. Chem. Soc. 111*, 8026.
Ryu, K., Stafford, D. R., & Dordick, J. S. (1989) *ACS Symp. Ser. 389*, 141.
Sakurada, J., Takahashi, S., & Hosoya, T. J. (1986) *J. Biol. Chem. 26*, 9657.
Sakurada, J., Sekiguchi, R., Sato, K., & Hosoya, T. (1990) *Biochemistry 29*, 4093.
Saunders, B. C., Holmes-Siedle, A. G., & Stark, B. P. (1964) *Peroxidase*, Butterworths, London.
Schejter, A., Lanir, A., & Epstein, N. (1976) *Arch Biochem. Biophys. 174*, 36.
Schulz, G. E., & Schirmer, R. H. (1979) *Principles of Protein Structure*, Springer-Verlag, New York.
Singer, S. J. (1962) *Adv. Protein Chem. 17*, 1.
Sorensen, J. M., & Arlt, W. (1980) *Liquid–Liquid Equilibrium Data Collection*, Vol. 3, Part 3, Chemistry Data Series, Dechema, Schon & Wetzel GmbH, Frankfurt.
Tanizawa, K., & Bender, M. L. (1974) *J. Biol. Chem. 249*, 2130.
Tanford, C. (1961) *Chemistry of Macromolecules*, Wiley, New York.

Teale, F. W. J. (1960) *Biochem. J. 76*, 381.
Thanabal, V., de Ropp, J. S., & La Mar, G. N. (1987) *J. Am. Chem. Soc. 109*, 7516.
Ugarova, N. N., Rozhkova, G. D., & Berezin, I. V. (1979) *Biochim. Biophys. Acta 570*, 31.
Weber, R. E., & Tanford, C. (1959) *J. Am. Chem. Soc. 81*, 3255.
Welinder, K. G. (1979) *Eur. J. Biochem. 96*, 483.
Wiberg, K. B. (1960) *Laboratory Technique in Organic Chemistry*, pp 240–251, McGraw-Hill, New York.
Yeoman, L. C., & Hager, L. P. (1980) *Biochem. Biophys. Res. Commun. 97*, 1233.
Zaks, A., & Klibanov, A. M. (1986) *J. Am. Chem. Soc. 108*, 2767.

Phosphonate Biosynthesis: Molecular Cloning of the Gene for Phosphoenolpyruvate Mutase from *Tetrahymena pyriformis* and Overexpression of the Gene Product in *Escherichia coli*[†,‡]

H. Martin Seidel, David L. Pompliano,[§] and Jeremy R. Knowles*
Departments of Chemistry and Biochemistry, Harvard University, 12 Oxford Street, Cambridge, Massachusetts 02138
Received October 9, 1991; Revised Manuscript Received December 16, 1991

ABSTRACT: The phosphoenolpyruvate mutase gene from *Tetrahymena pyriformis* has been cloned and overexpressed in *Escherichia coli*. To our knowledge, this is the first *Tetrahymena* gene to be expressed in *E. coli*, a task made more complicated by the idiosyncratic codon usage by *Tetrahymena*. The N-terminal amino acid sequence of phosphoenolpyruvate mutase purified from *T. pyriformis* has been used to generate a precise oligonucleotide probe for the gene, using in vitro amplification from total genomic DNA by the polymerase chain reaction. Use of this precise probe and oligo(T) as primers for in vitro amplification from a *T. pyriformis* cDNA library has allowed the cloning of the mutase gene. A similar amplification strategy from genomic DNA yielded the genomic sequence, which contains three introns. The sequence of the DNA that encodes 10 amino acids upstream of the N-terminal sequence of the isolated protein was found by oligonucleotide hybridization to a subgenomic library. These 10 N-terminal amino acids are cleanly removed in *Tetrahymena* in vivo. The full mutase gene sequence codes for a protein of 300 amino acids, and it includes two amber (TAG) codons in the open reading frame. In *Tetrahymena*, TAG codes for glutamine. When the two amber codons are each changed to a glutamine codon (CAG) that is recognized by *E. coli* and the gene is placed behind a promoter driven by the T7 RNA polymerase, expression in *E. coli* is observed. The mutase gene also contains a large number of arginine AGA codons, a codon that is very rarely used by *E. coli*. Cotransformation with a plasmid carrying the *dnaY* gene [which encodes $tRNA^{Arg}(AGA)$] results in more than 4-fold higher expression. The mutase then comprises about 25% of the total soluble cell protein in *E. coli* transformants. The mutase gene bears significant similarity to one other gene in the available data bases, that of carboxyphosphonoenolpyruvate mutase from *Streptomyces hygroscopicus*, an enzyme that catalyzes a closely related transformation. Due to the large evolutionary distance between *Tetrahymena* and *Streptomyces*, this similarity can be interpreted as the first persuasive evidence that the biosynthesis of phosphonates is an ancient metabolic process.

The enzyme phosphoenolpyruvate mutase (EC 5.4.2.9) catalyzes the first phosphorus–carbon bond-forming step in the biosynthesis of naturally-occurring phosphonates (Scheme I). For example, in the biosynthetic pathway that leads in *Streptomyces* to the herbicide bialaphos, the conversion of the phosphate ester in phosphoenolpyruvate (PEP) to the phosphonate in phosphonopyruvate is catalyzed by PEP mutase (Bowman et al., 1988; Seidel et al., 1988; Hidaka et al., 1989), while the reduction of the phosphonate to phosphinate (Scheme II) is catalyzed by a related enzyme, carboxyphosphonoenolpyruvate mutase (Hidaka & Seto, 1989; Hidaka et al., 1990). All compounds in nature containing a reduced form of phosphorus (that is, phosphonates or phosphinates) appear to owe their existence to PEP mutase or its congener.

Scheme I: PEP Mutase-Catalyzed Reaction

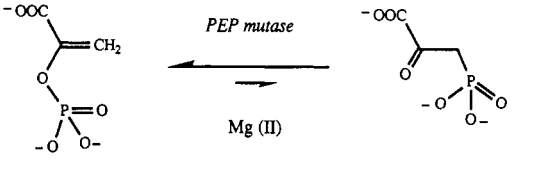

phosphoenolpyruvate (PEP) phosphonopyruvate

Scheme II: CPEP Mutase-Catalyzed Reaction

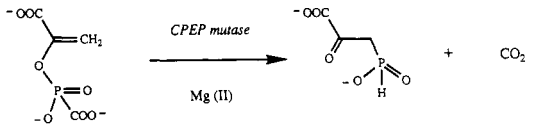

carboxyphosphonoenolpyruvate (CPEP) phosphinopyruvate

[†] Supported by the National Institutes of Health and the National Science Foundation and Eli Lilly (through predoctoral fellowships to H.M.S.).
[‡] The nucleotide sequence in this paper has been submitted to GenBank under accession number M85236.
* To whom correspondence should be addressed.
[§] Present address: Merck, Sharp & Dohme Research Laboratories, Department of Cancer Research, West Point, PA 19486.

0006-2960/92/0431-2598$03.00/0